Journal of Luminescence 159 (2015) 284–293

Contents lists available at ScienceDirect

Journal of Luminescence

journal homepage: www.elsevier.com/locate/jlumin

Thioflavin T derivatives for the characterization of insulin and lysozyme amyloid fibrils *in vitro*: Fluorescence and quantum-chemical studies

Kateryna Vus [a,*], Valeriya Trusova [a], Galyna Gorbenko [a], Rohit Sood [b], Paavo Kinnunen [b]

[a] Department of Nuclear and Medical Physics, V.N. Karazin Kharkiv National University, 4 Svobody Sq., Kharkiv 61022, Ukraine
[b] Department of Biomedical Engineering and Computational Science, School of Science and Technology, Aalto University, FI-00076 Espoo, Finland

ARTICLE INFO

Article history:
Received 24 June 2014
Received in revised form
17 September 2014
Accepted 20 October 2014
Available online 6 November 2014

Keywords:
Energy profile
Fluorescence
Insulin/lysozyme amyloid fibrils
Thioflavin T
Torsion angle
Viscosity

ABSTRACT

Two charged Thioflavin T (ThT) derivatives, referred to here as ICT2 and ICT3, showed higher fluorescence response, association constants and the blue-shifted emission maxima in the presence of lysozyme fibrils compared to insulin aggregates. In turn, the other two ThT derivatives, ICT4 and ICT5, possessed much weaker sensitivity to amyloid fibrils. Furthermore, a direct correlation was found between the "light-up" ability of the fibril-bound fluorophores and those observed in concentrated dichlormethane or glycerol solutions. To explain this behavior, the ground and lowest non-relaxed excited state properties of the dyes were evaluated with the 6-31G(d,p) basis set, using DFT and the CIS method. The excited state energy dependences along the torsion angle between the benzothiazole and phenyl moieties of the ICT4, ICT5 turned out to have three directly observed minima, corresponding to the locally excited (LE) and twisted intramolecular charge transfer (TICT) states. Thus, stronger stabilization of the ICT4, ICT5 LE states resulted in significantly greater quantum yield of these dyes in buffer solution and the absence of the "light-up" feature in the presence of insulin amyloid fibrils, compared to ICT2 and ICT3.

1. Introduction

Amyloid fibrils, a particular class of protein aggregates, attract ever-growing interest due to their crucial role in molecular etiology of numerous severe diseases, including neurological disorders, type II diabetes, systemic amyloidosis, etc. [1,2]. Morphologically, amyloid assemblies represent the bundles of twisted unbranched filaments composed of β-sheets with β-strands orthogonal to the long axis of the fibril [3,4]. These structural peculiarities allow to differentiate amyloid from other types of protein aggregates using a set of appropriate criteria [5–7]. One widespread criterion for identification of amyloid assemblies relies upon specific association of benzothiazole fluorescent dye Thioflavin T (ThT) with fibrillar structures [8,9], followed by significantly enhanced fluorescence and shift of ThT excitation maximum from 340 to 450 nm [10]. High efficiency of ThT criterion stimulated considerable research activity aimed at improving ThT analytical sensitivity and specificity [11–13].

To exemplify, interactions of ThT derivatives with Aβ amyloid fibrils have been extensively studied in an attempt to develop an ideal biomarker for Alzheimer's disease (AD) [14,15]. Some structural requirements for high binding affinity of amyloid targeting dyes have been uncovered, *viz.*, a neutral charge [16,17] and the presence of hydrogen bond donating substituents [18] or substituents with high polarizability and hydrophobicity on the benzothiazole and phenyl moieties [15,17]. These physicochemical peculiarities give rise to the enhancement of dispersion, hydrophobic and H-bonding interactions between the dye and β-sheet, which are supposedly responsible for the dye amyloid specificity [18]. In contrast, the presence of hydrogen bond donating groups on phenyl moiety, or replacement of phenyl ring with those of higher aromaticity resulted in lowered affinity for amyloid or the absence of any effects, respectively [13]. Besides, uncharged molecules showed up to 70-fold higher brain permeability than ThT, thus raising the possibility for improvement in the accuracy of AD diagnosis by positron emission tomography (PET) [14,19]. For instance, the neutral ThT derivative, Pittsburgh compound B, has been successfully employed to visualize AD amyloid pathology *in vivo* using the PET technique [20]. Interestingly, strong affinity of the dyes for Aβ amyloid fibrils turned out to inversely correlate with their "light-up" property [16,21], essential for *in vitro* amyloid detection by fluorescence techniques and *in vivo* multiphoton microscopy imaging of amyloid deposits [14,16]. Only ThT dimers (diThT) displayed strong affinity for Aβ-fibrils coupled with

* Correspondence to: 38-12 Aeroflotskaya Str., Kharkiv 61031, Ukraine. Tel.: +380 57 3438244; fax: +380 57 7544746.
E-mail address: kateryna_vus@yahoo.com (K. Vus).

http://dx.doi.org/10.1016/j.jlumin.2014.10.042
0022-2313/

pronounced fluorescence response [19], although high molecular weight and charge of diThT was suggested to limit brain entry of this compound [22].

Since fluorescence spectroscopy and microscopy have been prized as very informative techniques due to their inherent sensitivity, good spatial and temporal resolution, atomic level studies assisting in rational design of ThT-based amyloid markers with strong "light-up" properties are of considerable interest [23]. Notably, the photophysical properties of ThT are determined by its donor–π–acceptor architecture, where an electron donating substituent on the phenyl ring is connected to the benzothiazole electron acceptor through a π-electron rich bridge [24]. The excitation of the dye in low viscosity solvents induces an intramolecular charge transfer (ICT) and relative rotation of the phenyl and benzothiazole rings, thus leading to the formation of the non-fluorescent twisted intermolecular charge transfer state (TICT) [10,25]. In turn, de-excitation of ThT occurs from the locally excited (LE) state in glycerol-water solutions [26] and in the presence of amyloid fibrils [27], leading to enhancement of the dye quantum yield up to ~1000 times due to rotational lock induced by viscous solvents. In other words, this compound shares common features with molecular rotors, such as DCVJ [28] and Nile Red [29], i.e., low sensitivity to microenvironmental polarity and strong fluorescence enhancement in viscous solvents. Thus, it seems likely that fluorescence response of ThT derivatives in the presence of amyloid fibrils is also governed by the properties of LE and TICT states (*viz.*, energies [30], dipole moments [31], etc.) depending on the substituents on benzothiazole and phenyl moieties. For example, a neutral dye, BTA-2, possessing higher affinity and lower "light-up" ability in the amyloid Aβ-incorporated form than those of the parent compound, may have lower tendency to form the fully twisted conformation upon excitation due to similar energies of LE and TICT states [25]. This can provide an explanation for high quantum yield of this compound in buffer solution, and consequently, reduction of the fluorescence response in the presence of amyloid fibrils [16]. Thus, photophysical characteristics of ThT derivatives may have essential impact on their environmental sensitivity [32]. Notably, it cannot be excluded that fluorescence of neutral ThT analogs in nonpolar solvents may become stronger compared to their charged counterparts, raising the probability of their incorporation into hydrophobic pockets of native proteins and reducing their selectivity to amyloid fibrils. Additionally, nonpolar solvents, similar to hydrophobic surfaces of native proteins, cannot compensate positive charge of ThT (and charged ThT analogs) and stabilize the TICT state, thereby enhancing the sensitivity of the dyes to viscous environment (e.g., fibrillar aggregates) [33]. Therefore, the investigation of the charged Thioflavin T analogs is of interest, although they could be employed only for the *in vitro* studies, where a fresh dye sample is used there for the analysis. It is due to the high rate of Thioflavin T hydroxylation at alkaline pH and high temperature that greatly restricts the dye application for *in situ* studies [34,35].

To get deeper insight into the effect of different substitutions in the benzothiazole moiety on the dye spectral properties and affinity for protein aggregates, which could help in more rational design of the amyloid markers, we compared fluorescence and quantum-chemical characteristics of four recently synthesized positively charged Thioflavin T derivatives with those of Thioflavin T. Specifically, our goal was several fold: (i) to evaluate fluorescence response and the parameters of the dye binding to insulin, lysozyme amyloid fibrils; (ii) to find out whether the probes under study could be used as alternatives to Thioflavin T for amyloid fibril characterization; (iii) to give a quantum-chemical characterization of the ground and excited states of the examined ThT analogs in order to find out to what extent their photophysical behavior is determined by TICT state formation upon excitation; and (iv) to provide a comparative description of the photophysical properties of the free and protein-bound dyes based on the experimental data and theoretical calculations.

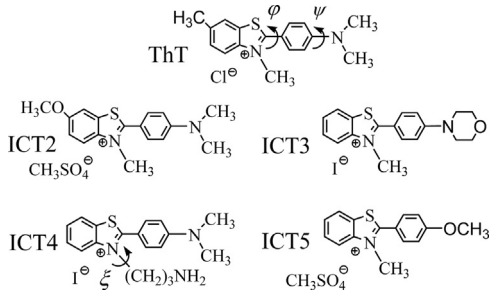

Fig. 1. Structural formulas of Thioflavin T and its derivatives.

2. Materials and methods

2.1. Materials

Insulin from bovine pancreas and hen egg white lysozyme were purchased from Sigma (St. Louis, MO, USA). Thioflavin T and glycerol (GL) were from Sigma (Steinheim, Germany). ThT derivatives (Fig. 1), referred to here as ICT2, ICT3, ICT4 and ICT5, were recently synthesized by Dr. Nedyalko Lesev and Dr. Stefka Kaloyanova (Faculty of Chemistry of St. Kliment Ohridski University of Sofia), as described previously [36,37]. 1-anilinonaphthalene-8-sulfonic acid (1,8-ANS) was from Molecular Probes (Oregon, USA). Dichlormethane (DCM) and N,N-dimethylformamide (DMF) were purchased from MERCK (Darmstadt, Germany). Stock solutions of the fluorophores were prepared by dissolving the dyes in 5 mM sodium phosphate buffer. The dye concentrations were determined spectrophotometrically using the extinction coefficients at absorption maximum (Table 1, λ_{abs}^{buf}) 7'700, 13900, 15100, 16000 and 23'800 M^{-1} cm^{-1} for ICT2, ICT3, ICT4, ICT5 and ThT, respectively.

2.2. Preparation of insulin and lysozyme fibrils

Insulin/lysozyme fibrillization was induced by continuous shaking of the protein solution (10/60 mg/ml) in 10 mM glycine buffer (pH 1.6) for 10/14 days at 37/65 °C [38,39]. The amyloid nature of insulin fibrillar aggregates was confirmed by transmission electron microscopy (Fig. 2A). The fibrillization of lysozyme was monitored using the Thioflavin T assay: aliquots (10 μl) of protein stock

Table 1
Spectral properties of Thioflavin T derivatives in buffer solution and their fluorescence response in the presence of insulin and lysozyme amyloid fibrils.

Dye	λ_{abs}^{buf} (nm)	λ_{InsF} (nm)	λ_{LzF} (nm)	Q_{buf}*10^4	I_{InsF} / I_{buf}	I_{LzF} / I_{buf}	I_{GL} / I_{DMF}	I_{DCM} / I_{DMF}	I_{GL} / I_{DCM}
ThT	412	488	483	1	116	14.0	99	7.2	14.0
ICT2	397	497	484	7	7	1.5	12	1.7	7.4
ICT3	388	493	488	4	18	2.7	57	6.6	9.0
ICT4	*362 (417)	435	428	3880	0.7	1.0	1	0.8	1.2
ICT5	328	436	426	950	1.0	0.94	1.9	1.2	1.6

* The absorption spectrum of ICT4 had a shoulder at 417 nm.

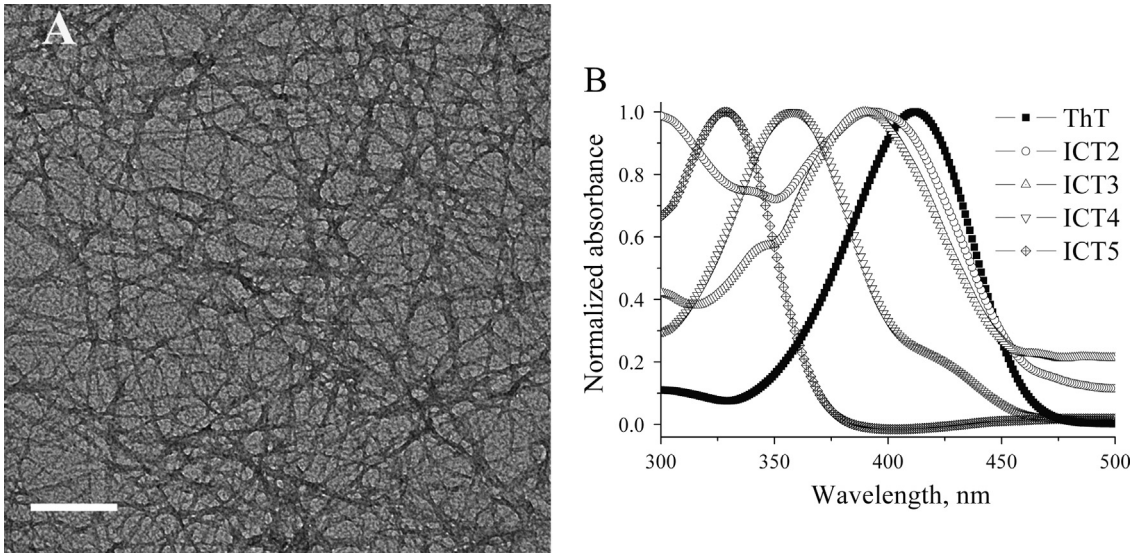

Fig. 2. Visualization of insulin amyloid fibrils by TEM. Scale bar is 200 nm (A). Normalized absorbance of ICT2, ICT3, ICT4, ICT5 and ThT in buffer (B).

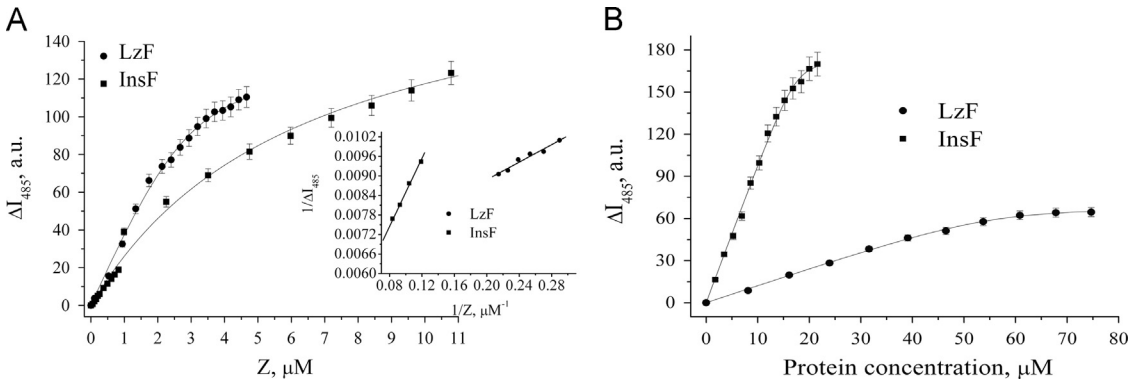

Fig. 3. ICT2-fibril binding isotherms obtained by measuring the increase in the dye fluorescence intensity at 485 nm relative to that in buffer upon protein titration by the fluorophore. Inset figure represents the double reciprocal plots of the isotherms. Insulin and lysozyme concentrations were 7 and 16 μM, respectively (A). The increase in ICT2 fluorescence intensity at 485 nm as a function of the protein concentration. ICT2 concentration was 1 μM (B).

solution were withdrawn during the incubation period and mixed with 2 ml of Thioflavin T solution (17 μM). ThT fluorescence was excited at 420 nm, and lysozyme fibrillization resulted in ~30-fold increase of the dye fluorescence at 485 nm.

2.3. Transmission electron microscopy

For electron microscopy assay, a 5 μl drop of the protein solution (diluted 10 times) was applied to a carbon-coated grid and blotted after 1 min. A 10 μl drop of 2% (w/v) uranyl acetate solution was placed on the grid, blotted after 30 s, and then washed 3 times by deionized water and air dried. The resulting grids were viewed at Tecnai 12 BioTWIN electron microscope.

2.4. Steady-state fluorescence measurements

Steady-state fluorescence spectra of the dyes were recorded at 20 °C with Varian Cary Eclipse (Varian Instruments, Walnut Creek, CA) spectrofluorimeters equipped with a magnetically stirred, thermostated cuvette holder, using 10 mm path-length quartz cuvettes. The excitation and emission slit widths were set at 10 nm. ICT2, ICT3, ThT were excited at 420 nm. ICT4, ICT5 were excited at 362 and 328 nm, respectively (Fig. 2B). Notably, the emission maxima of ICT4 excited at 362 or 420 nm were *ca.* 438 nm, and the former excitation wavelength was selected to avoid light scattering. The emission maxima of the fibril-incorporated dyes are given in Table 1. 1,8-ANS was excited at 372 nm and the dye emission was collected at 480 and 473 nm, corresponding to the fluorescence of the insulin and lysozyme fibril-bound dye, respectively. Fluorescence response of the probes in the presence of insulin fibrils, or relative intensity increase of each dye (5 μM) bound to fibrillar protein (7.1 μM), was defined as I_{InsF}/I_{buf} (I_{LzF}/I_{buf}) (Table 1), where I_{buf} and I_{InsF} (I_{LzF}) are the dye fluorescence intensities in buffer solution and in the presence of protein aggregates, respectively. Sensitivity of the new probes (5 μM) to the solvent polarity or viscosity was evaluated using the following expressions: I_{GL}/I_{DMF}, I_{GL}/I_{DCM}, and I_{DCM}/I_{DMF} (Table 1), where I_{GL}, I_{DMF} and I_{DCM} are the dye fluorescence intensities in GL (~98%, $\eta \approx 939$ mPa·s, $\varepsilon \approx 42.5$), DMF ($\eta \approx 0.92$ mPa·s, $\varepsilon \approx 37.8$) and DCM ($\eta \approx 0.4$ mPa·s, $\varepsilon \approx 8.9$), respectively. The fluorescence intensities (I_{InsF}, I_{LzF}, I_{buf}, I_{GL}, I_{DCM}, and I_{DMF}) at 485 nm (for ICT2, ICT3 and ThT), 428 nm (for ICT4) and 426 nm (for ICT5) were used for the above calculations. The measured fluorescence intensity of each dye was corrected to the absorption at the excitation wavelength. Besides, the quantum yield of the dyes in buffer solution (Table 1, Q_{buf}) was evaluated as described previously [40], using ThT as a reference dye ($Q_{buf} \approx 0.0001$) [26].

2.5. Binding studies

Association constants (K_a) and stoichiometry (n) for the dye–protein binding were estimated from the fluorimetric titration of insulin (or lysozyme) amyloid fibrils by ICT2, ICT3 and ThT (Fig. 3A)

Table 2
Binding characteristics of the novel Thioflavin T derivatives and Thioflavin T associated with insulin and lysozyme fibrils.

Protein	Insulin			Lysozyme		
Dye	K_a (μM^{-1})	n	α (μM^{-1})	K_a (μM^{-1})	n	α (μM^{-1})
ThT	1.80	0.005	6119	4.9	0.06	891
ICT2	0.06	0.245	176	0.8	0.26	39
ICT3	0.11	0.057	1014	3.1	0.02	208

using the one-site Langmuir adsorption model. Linear approximation of the double reciprocal plots $1 / \Delta I_{485}$ (ΔI_{485} – fluorescence intensity increase at 485 nm) vs. $1 / Z$ (Z – total dye concentration) allowed us to determine the K_a values (Fig. 3A, inset figure) [41,42]. For the determination of the value of n we performed the titration of the dyes by the protein aggregates (Fig. 3B), giving the value of α – a coefficient proportional to the difference of the dye quantum yield in a buffer solution and protein-associated state. Finally, we calculated the value of n using the α value and the plot $1 / \Delta I_{485}(1 / Z)$ as described previously [43]. The resulted binding parameters are presented in Table 2.

2.6. Quantum-chemical calculations

Semiempirical AM1 method [44] with added polarization (1) and diffuse (1) functions on heavy atoms, and a polarization function on hydrogen atoms was employed for the ground state S_0 geometry optimization of the ThT derivatives. This method is thought to provide reasonable geometries and potential energy dependences on the torsion angles, together with relatively low computational cost [45,46]. The resulted geometries of the fluorophores were further used as starting conformations for calculation of the ground state energies with 6-31G(d,p) basis [47]. Furthermore, a more accurate description of the ground state, dipole moments and charges of the conformers corresponding to selected points of the potential energy profiles was performed with the 6-31G(d,p) basis set, using density functional theory (DFT) and B3LYP functional [48], offering reasonable estimates of the ground state properties [49]. Dipole moments and charges of the non-relaxed excited states S_1^{abs} (the upper index "abs" denotes the lowest singlet excited state, formed immediately after photon absorption) occurring immediately after excitation of the dyes, the excited state energies and oscillator strengths of the $S_0 \rightarrow S_1^{abs}$ electronic transition were obtained with 6-31G(d,p) basis, using time-dependent density functional theory (TDDFT) and B3LYP functional [45,50]. Alternatively, dipole moments and charges of S_1^{abs} were calculated with CIS/6-31G(d,p) [51], although the CIS method was shown to underestimate dipole moments and bond lengths of diatomic molecules [52]. In turn, the excited state energies and other properties of coumarins [53] and other organic compounds [54,55] calculated with TDDFT were reported to be of high quality. HOMO and LUMO shapes of the dyes were obtained using geometry optimization with the 3-21G basis set.

All calculations were performed in the gas phase using WinGamess (version May 1, 2013 R1) [56]. Molecular orbitals of the dyes were visualized by MacMolPt, designed for Gamess output visualization [57].

3. Results and discussion

3.1. Fluorescence response of the ThT derivatives to the presence of insulin and lysozyme fibrils

Typical fluorescence spectra of the examined ThT analogs in a free and fibril-bound states are presented in Fig. 3. As shown in the insets, ThT fluorescence response (I_{InsF} / I_{buf} and I_{LzF} / I_{buf}) in the presence of amyloid fibrils is 6.4–166-fold higher compared to that of the ThT derivatives. Notably, the emission maxima of lysozyme-incorporated ThT derivatives are *ca.* 5–13 nm shifted to the shorter wavelengths (Table 1, λ_{InsF} and λ_{LzF}), that is presumably resulted from the lower polarity of lysozyme fibrillar aggregates. Indeed, the surface hydrophobicity of lysozyme fibrils appeared to be higher than that of insulin aggregates due to the larger "blue" emission shifts and "light-up" abilities of the lysozyme-bound ANS, as well. Specifically, 1,8-ANS (5 μM) showed the blue shift of the emission maximum and the "light-up" ability *ca.* 46 (51) nm and 4.7 (39), respectively, in the presence of insulin (lysozyme) amyloid fibrils (7.1 μM). This is indicative of the presence of nonpolar binding sites for the probes (i.e., the solvent-exposed hydrophobic patches) on the fibril (or protofibril) surface [58,59], while few amorphous aggregates of insulin (Fig. 2A) and lysozyme [39,60] prepared using the rapid and highly efficient "agitation-heating" method, were detected by TEM. Notably, our findings are consistent with the previous study of *in vitro* prepared insulin and lysozyme fibril structures by Mishra et al. [29]. In turn, ICT4 and ICT5 showed the highest fluorescence quantum yield in buffer solution and no "light-up" abilities in the presence of amyloid fibrils (Table 1, Q_{buf}). Interestingly, the association constants of ICT2- and ICT3–lysozyme interactions were stronger than those for the dye–insulin complexes, presumably due to the higher hydrophobicity and aromaticity of the lysozyme fibril grooves, serving as the binding sites for the dyes [27]. Furthermore, the spectral responses of ICT2, ICT3 and ThT in the presence of insulin amyloid fibrils turned out to be 5–8 times stronger than those in the presence of lysozyme aggregates (Table 1), in spite of the lower surface hydrophobicity of insulin fibrils. This effect has been also observed in previous studies for the insulin and lysozyme-incorporated ThT [61] and Nile Red [29], and could occur, in turn, due to high steric restrictions for the intramolecular rotation of the insulin-bound probes, which fluorescence intensity seems to be sensitive to the solvent viscosity, as well [62]. In this case, ICT2 and ICT3 could be employed for amyloid detection and distinguishing between the protein aggregates of different viscosity. Interestingly, bovine insulin and hen lysozyme fibrils prepared under similar conditions (10 mg/ml, pH 2, incubation at 60–70 °C up to 14 days, no agitation) [63,64] showed the values of the *bending rigidity* (i.e., a physical property of amyloid fibrils, which depends on a generic inter-backbone hydrogen-bonding network [64]) *ca.* $\sim 9.1 \times 10^{-26}$ and 4×10^{-26} N · m^2, which translated into the persistence lengths of *ca.* ~22 [64] and 8.9 μM [63,65], respectively. Furthermore, the insulin fibrils prepared at pH 2, high temperature and under agitation were *ca.* 10–50 nm in diameter and composed of 2–6 filaments [66,67]. In turn, lysozyme aggregates formed in a similar way had the diameter *ca.* 7–20 nm and were composed of 2–3 filaments [60,68]. To conclude, the resulting structure of lysozyme fibrils could possess lower rigidity than that of insulin fibrils due to (i) a positive correlation between the persistence length and the number of fibril filaments [65,69] and (ii) possible additional constraints associated with the packaging of longer lysozyme polypeptide chain into the cross-β amyloid core [63].

Based on the above experimental data we supposed that different relative fluorescence responses of the fluorophores (Fig. 4) depend on the varied sensitivity to the environmental factors. Therefore, at the next step of the study we evaluated the sensitivity of the dyes to solvent polarity and viscosity. It appeared that I_{GL} / I_{DMF} values (Table 1) were the highest for ThT and ICT3 (*ca.* 99 and 57, respectively), i.e., the strongest fluorescence was observed for these dyes in GL compared to that in DMF (the solvent with similar dielectric constant to that of GL). Furthermore, the strong correlation (k=0.91) was observed between I_{InsF} / I_{buf} (I_{LzF} / I_{buf}) and I_{GL} / I_{DMF} values, while a comparatively weak correlation (k=0.76) was found between I_{InsF} / I_{buf} (I_{LzF} / I_{buf}) and I_{DCM} / I_{DMF} ratios. The above results

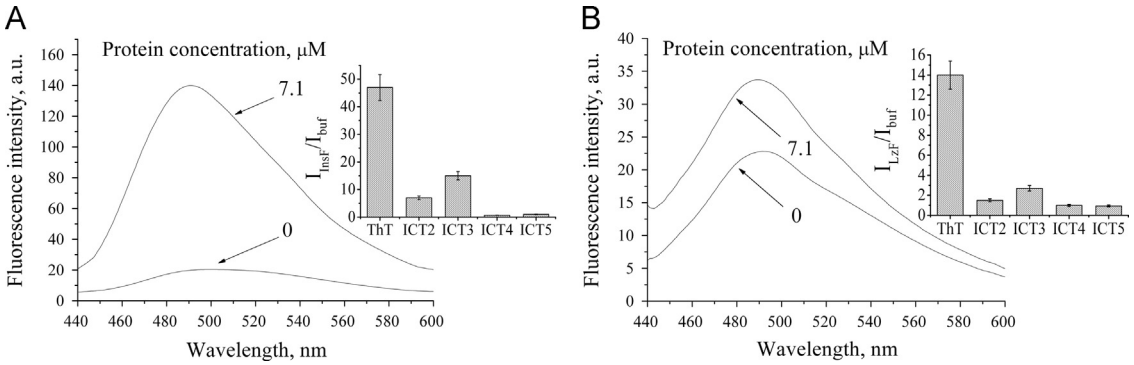

Fig. 4. Fluorescence spectra of 5 μM ICT2 in buffer and in the presence of 7.1 μM fibrillar insulin (A) and lysozyme (B). Inset figures represent relative fluorescence responses (I_{InsF}/I_{buf} or I_{LzF}/I_{buf}) of the dyes (5 μM).

Table 3
S_0 and S_1^{abs} state energies, dipole moments, benzothiazole charges and oscillator strengths of the Thioflavin T derivatives at $\varphi = \varphi_{min}$.

Dye	$E_{S0(\varphi=0)} - E_{S0(\varphi=\varphi_{min})}$ (cm^{-1})	ΔE_{S1}^{abs} (cm^{-1}, nm)	μ_{S0} (D)	μ_{S1}^{abs} (D)	q_{S0}	q_{S1}^{abs}	$f(\varphi=\varphi_{min};\ \varphi=0)$
ThT	1218	24,399, 410	2.3	6.5	0.59	0.42	0.80; 1.00
ICT2	1208	24,117, 415	3.7	6.1	0.60	0.46	0.86; 0.99
ICT3	1272	24,326, 411	5.4	2.7	0.59	0.34	0.79; 0.96
ICT4	1864	22,955, 436	2.0	9.3	0.63	0.36	0.49; 0.89
ICT5	1578	27,561, 363	2.1	3.8	0.65	0.43	0.61; 0.71

point to the correlation between the dye affinity for amyloid fibrils and their sensitivity to both polarity and viscosity. Indeed, ICT2, ICT3, ThT had a good sensitivity to the environmental factors and the presence of amyloid fibrils, while ICT4, ICT5 showed the lowest sensitivity to both solvent polarity/viscosity and protein aggregates. Furthermore, I_{DCM} values of the examined probes appeared to be *ca.* 1.2–14 times lower than I_{GL} (Table 1, I_{GL} / I_{DCM}) pointing to prevailing sensitivity of the dye fluorescence intensity to solvent viscosity rather than its polarity. These results allowed us to propose an explanation for the lower fluorescence response of the ThT derivatives to the presence on insulin amyloid fibrils compared to ThT, as well. Specifically, the weaker sensitivity of ICT2, ICT3, ICT4 and ICT5 to solvent viscosity (Table 1, I_{GL} / I_{DMF}) could be the major reason for the observed phenomenon. In other words, the above correlations indicate that the novel probes could share the properties of the molecular rotors similarly to ThT [25] and DCVJ [28], although these features are weaker compared to that of the classical fluorescent amyloid marker.

Notably, the ICT3 and ICT2 viscosity sensitivities (I_{GL} / I_{DMF}) were *ca.* 1.7 and 8.3 times weaker than that of ThT, and the "light-up" abilities of the novel probes – I_{InsF} / I_{buf} (I_{LzF} / I_{buf}) appeared to be *ca.* 6.4 (4.7) and 16.5 (8.7) times lower, respectively. This may indicate that apart from the environmental factors, lower dye–protein binding parameters could also lead to the weaker "light-up" features of the novel dyes in the presence of insulin amyloid fibrils compared to ThT. Indeed, the association constants of ICT2 and ICT3 appeared to be 1.6–30 times higher than the corresponding parameter for ThT (Table 3). ThT exhibits stronger affinity for the protein aggregates than the novel probes, since it bears CH_3 group at sixth position that was reported to play essential role in the dye positioning on β-sheet surface due to minimizing dye-fibril steric repulsion [14]. In turn, ICT2 and ICT3 could have the lower affinity for the protein aggregates (Table 1, K_a) due to repulsion of the metoxy substituent at sixth position of the benzothiazole moiety and the carbonyl oxygens of the β-sheets [18] or due to the presence of the bulky substituent at 4′-position [13], respectively.

The fact that the novel dyes, especially ICT4 and ICT5, did not display better amyloid-detecting ability than ThT (i.e. possess low viscosity sensitivity) can be attributed to the differences in photophysical properties of these dyes, as well. In particular, stronger emission of the fluorophores in buffer solution may result from: (1) higher energy barrier for intramolecular rotation from LE to the TICT state, that reduces the population of TICT state upon excitation [25] and (2) lower-lying energy levels of the LE states of the novel dyes, compared to the TICT states, that stabilizes the LE state and prohibits the TICT state formation.

The first phenomenon may occur due to the preference of planar (or nearly planar) dye conformation for excited state, if the twisting around donor-acceptor bond is hindered by (i) steric interactions (like in the compound 20 [70]), or (ii) additional bridges between the donor and acceptor (similar to the compounds 214 and 216, 234 and 235, 244 and 245), as reviewed by Grabowski et al. [70]. The latter, however, could not account for high quantum yield of the novel dyes because of the absence of any additional bonds between the benzothiazole and phenyl rings in the fluorophore structures (Fig. 1), in contrast to ThT derivatives bearing an intramolecular hydrogen bond (e.g., compounds 5a, 6a, 7a reported by Ali-Torres et al.) and thus possessing a planar conformation [18]. In turn, steric restrictions and high ground state dipole moments may suppress mutual twisting of the donor and acceptor moieties of the dyes [30]. These restrictions could lead to rather high quantum yield of ICT4 in buffer solution (Table 1, Q_{buf}).

The second phenomenon was suggested to occur due to lowering of the donor capability and acceptor strength of the donor and acceptor moieties, respectively, promoting the formation of highly fluorescent LE state instead of TICT state of the probes [71,72]. For example, a xanthene dye showed strongly elevated quantum yield in acidic medium compared to that observed at pH 7.4, while protonation of the aniline lone pair reduced its donor capability. In general, if the donor ability is weakened, the dyes are not expected to populate the TICT state even in a rigid perpendicular conformation, in which the energy of TICT state appears to be much higher than that of LE state [71]. Indeed, lower donor capabilities of the morpholino and metoxy substituents on the phenyl rings of ICT3 and ICT5, respectively, compared to those of ThT dimethylamino moiety, could be responsible for their brighter fluorescence in

buffer solution because of the increased TICT state energy level relative to LE state. In turn, the electron-donating metoxy substituent on the benzothiazole ring of ICT2 probably reduces the accepting power of this moiety, leading to the increased quantum yield of the probe compared to ThT (Table 1, Q_{buf}) [71].

Notably, hydrogen bond formation between the examined compounds and the solvent [70,73], or excimer formation [31] may hardly occur at low dye concentrations in a polar aprotic environment. Therefore, these processes were suggested to exert no influence on the stability of LE or TICT states.

3.2. Quantum-chemical calculations of the ground state energy profiles of ThT derivatives

In order to explain the different behavior of ICT2, ICT3, ThT and ICT4, ICT5, observed experimentally, it seemed reasonable to investigate the effects of torsional motion of benzothiazole and phenyl rings on the photophysical properties of the dyes using quantum-chemical calculations. First, we examined the ground state potential energy profiles of the dyes along the torsion angles φ, ψ and ξ (Fig. 1) with the AM1 method. It appeared that local energy minima corresponding to the ICT2 conformers with φ=37°, 143°, 217°, and 323° are separated by the low and equivalent energy barriers *ca.* ~650 cm^{-1} (Fig. 5A). Notably, AM1 was believed to have reasonable accuracy for the quantum-chemical study of ThT derivatives, because the potential energy dependences and the energy barriers between neighboring minima, calculated with this method, had similar shapes and magnitudes, respectively (data not shown) with those obtained for ThT by Stsiapura et al. [24]. The more accurate estimates for the energy barriers obtained using the 6-31G(d,p) basis set are shown in Tables 3 and 4 ($E_{S0(\varphi=0)}-E_{S0(\varphi=\varphi_{min})}$ and $E_{S0(\varphi=90)}-E_{S0(\varphi=\varphi_{min})}$, correspond to the barriers for adopting a planar (φ=0°) or fully twisted (φ=90°) conformation, respectively). Our results indicate that the optimized geometries of the dyes are somewhat twisted ($\varphi_{min}=34-49°$) presumably due to steric interactions of methyl group of the benzothiazole moiety with hydrogen atoms of the phenyl ring [24]. Interestingly, the highest $E_{S0(\varphi=0)}-E_{S0(\varphi=\varphi_{min})}$ and rather high $E_{S0(\varphi=90)}-E_{S0(\varphi=\varphi_{min})}$ values were found for ICT4 with TDDFT(B3LYP)/6-31G(d,p) (Tables 3 and 4). This indicates that ICT4 do not favor the fully twisted (or planar) form in the ground state due to steric constraints between the propylamine substituent on the benzothiazole ring and hydrogen atoms of the phenyl moiety. In general, the energy barriers for fully twisted or planar conformation of the dyes in the ground state were similar and not very high (Tables 3 and 4).

Likewise, the energy dependences of the conformers on the torsion angle ψ turned out to have minima at ψ=0, 180, 360° due to the conjugation effects (Fig. 5B) [24]. Interestingly, these profiles were similar for all dyes (except of ICT5) (*ca.* 2100–2600 cm^{-1}). The ICT5 energy dependence on ψ appeared to have a symmetrical shape, indicating that planarity of the metoxy group does not depend on its rotation relative to the phenyl ring [24]. Finally, the energy profile of ICT4 along ξ showed two minima at $\xi\approx50°$ and $\xi\approx300°$, separated by the $E_{S0(\varphi=90)}-E_{S0(\varphi=\varphi_{min})}$ barrier *ca.* 1500 cm^{-1} (data not presented). Based on the quantum-chemical calculations of the potential energy profiles we concluded that internal rotation induced by the changes in the torsion angles ψ and ξ (for ICT4), can hardly lead to the TICT state formation. This is due to the 2–4-fold higher energy "humps" corresponding to these torsional motions, compared to the barriers for relative rotation of the benzothiazole and phenyl moieties (along φ). Our suggestion is supported, particularly, by the fact that mutual twisting of dimethylamino group and phenyl ring around the C–N bond (corresponding to the torsion angle ψ) in Rhodamine dyes (compounds 242 and 241) induced two orders of magnitude slower fluorescence quenching channel, than rotation of the whole aniline group [70]. Moreover, rotation of the dimethylamino group around the phenyl ring was not involved in the formation of TICT state in the donor-acceptor systems with quinoxaline as acceptor (compounds 142 and 144) [70]. In the following, we limited the calculations to the

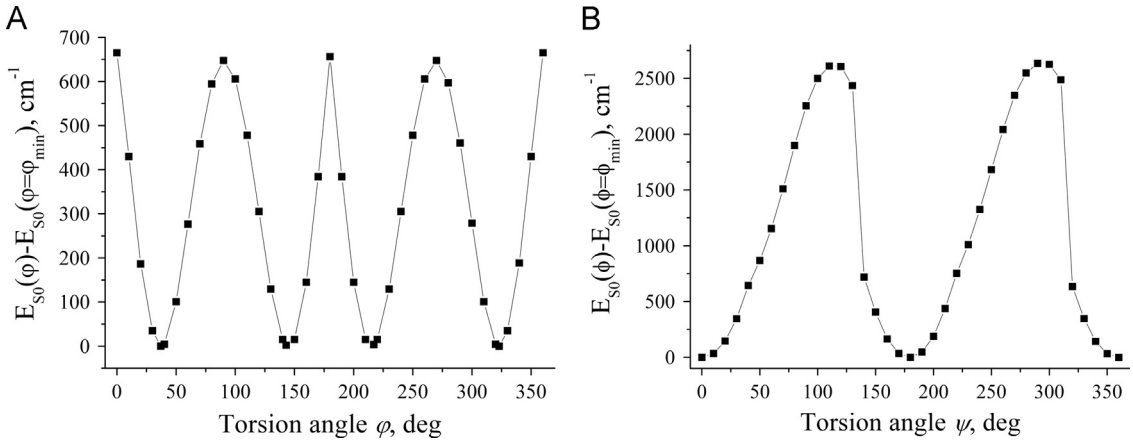

Fig. 5. The ground state energy dependences of ICT2 on φ (A) and ψ (B) torsion angles. Calculations were performed with the AM1 method, including an additional polarization function on H-atoms, 1 polarization and 1 diffuse functions on heavy atoms.

Table 4
S_0 and S_1^{abs} state energies, dipole moments, benzothiazole charges and oscillator strengths of the Thioflavin T derivatives at φ =90.

Dye	$E_{S0(\varphi=90)}-E_{S0(\varphi=\varphi_{min})}$ (cm^{-1})	ΔE_{S1}^{abs} (cm^{-1}, nm)	μ_{S0} (D)	μ_{S1}^{abs} (D)	q_{S0}	q_{S1}^{abs}	f
ThT	1748	17'632, 567	2.5	16.2	0.71	0.12	0.00
ICT2	1651	17'809, 562	3.3	17.5	0.72	0.12	0.00
ICT3	1731	17'774, 564	8.3	10.6	0.72	0.12	0.00
ICT4	1717	17'640, 567	1.6	16.3	0.71	0.12	0.00
ICT5	1077	23'568, 424	4.0	12.2	0.74	0.16	0.00

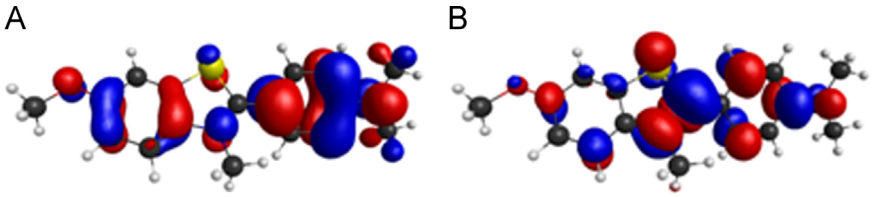

Fig. 6. HOMO-79 of ICT2 (A) and LUMO-80 of ICT2 (B). The optimzed conformations of the dyes were calculated with the 3-21G basis set.

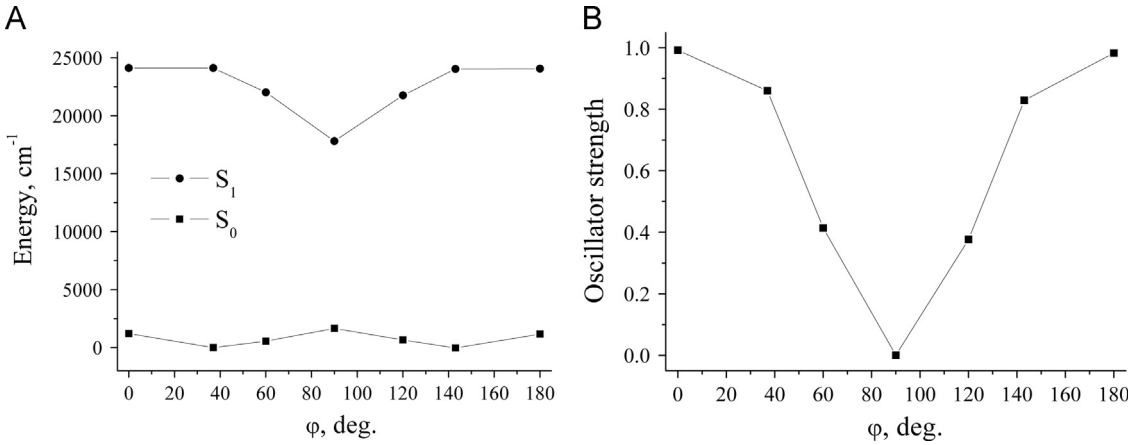

Fig. 7. Quantum chemical characteristics of the ground S_0 and first excited S_1^{abs} states of ICT2 conformers with different φ angles. Calculations were implemented using the ground state geometries optimized with the AM1 method, including an additional polarization function on H-atoms, 1 polarization and 1 diffuse functions on heavy atoms. Energies of the ground ($E_{S0(\varphi)} - E_{S0(\varphi=\varphi_{min})}$,) and excited ($\Delta E_{S1}^{abs}$) states (A) and oscillator strengths for the first electronic transition $S_0 \rightarrow S_1^{abs}$ (B) were calculated with DFT (TDDFT)/B3LYP/6-31G(d,p).

interval $\varphi = 0 - 180^{\circ}$ because of symmetric forms of the potential energy surfaces (Fig. 5A).

3.3. *Photophysical properties of the ground and the lowest singlet excited states of Thioflavin T derivatives*

At the next step of the study, HOMO and LUMO shapes were calculated using the geometry optimization of the dyes with the 3-21G basis set (Fig. 6). These shapes were similar to those obtained for ThT and indicate that $S_0 \rightarrow S_1^{abs}$ electronic transitions of the dyes are $\pi \rightarrow \pi^*$ in nature [24,74]. Furthermore, the calculations of the ground/excited state dipole moments (μ_{S0} / μ_{S1}^{abs}), benzothiazole charges (q_{S0} / q_{S1}^{abs}), excited state energies (ΔE_{S1}^{abs}) and oscillator strengths (f) for the electronic transitions $S_0 \rightarrow S_1^{abs}$ of the conformers with the fixed φ angles, were performed with TDDFT(B3LYP)/6-31G(d,p) (Figs. 7 and 9). Presented in Tables 3 and 4 are the results obtained for the conformers with $\varphi = \varphi_{min}$ and $\varphi = 90^{\circ}$. Notably, the properties of the non-relaxed excited states S_1^{abs} were estimated with fluorophore geometries being optimized in the ground state. The data acquired with CIS/6-31G(d,p) and TDDFT(B3LYP)/6-31G(d,p) (Tables 3 and 4) proved to be close to the results of Stsiapura et al. obtained using CIS/3-21G and INDO/S, respectively [24]. However, the ΔE_{S1}^{abs} values of fully twisted ThT derivatives were *ca.* 20% lower compared to those obtained for ThT with the INDO/S method [24]. Additionally, the energies of the vertical electronic transitions of the dyes were close to those observed experimentally, although somewhat underestimated (Tables 1, λ_{abs}^{buf} and 4, ΔE_{S1}^{abs}). Interestingly, the excited state dipole moments of ICT3 and ICT5 calculated with CIS/6-31G(d,p) turned out to be lower than those of the ground state (data not presented). The same results were obtained for organic chromophores, as reported e.g., by Keinan et al. [75]. The calculations performed with TDDFT(B3LYP)/6-31G(d,p) yielded somewhat improved estimates, although the μ_{S1}^{abs} value of ICT3 remained lower than μ_{S0} at $\varphi = \varphi_{min}$ (Tables 3 and 4). Therefore, μ_{S1}^{abs} and q_{S1}^{abs} values estimated with TDDFT(B3LYP)/6-31G(d,p) were used for comparative analysis of the photophysical properties of the dyes, although CIS/6-31G(d,p) and TDDFT(B3LYP)/6-31G(d,p) gave almost identical μ_{S1}^{abs} and q_{S1}^{abs} profiles along the torsion angle φ (Fig. 8). In general, the methods employed in this study seem to have reasonable accuracy for the calculation of the quantum-chemical properties of the examined ThT derivatives.

As seen in Fig. 7A, the energy of ICT2 first singlet excited state has a minimum at $\varphi = 90^{\circ}$, raising the probability of rotation of the benzothiazole and phenyl moieties relative to each other (i.e. when the torsion angle φ changes from 37°, corresponding to minimum of the ground state energy profile, to 90°). In turn, the fully twisted dye conformation may lead to the disappearance of π-conjugation between the benzothiazole and phenyl rings and thus to complete nulling of the oscillator strength (emission from this state is not allowed due to the "minimum overlap" rule) (Fig. 7B) [72]. Moreover, ICT2 dipole moments display increase, while benzothiazole charges tend to decrease upon excitation (Fig. 7). Specifically, the largest q_{S1}^{abs} value was found for the dye conformer with $\varphi = 90^{\circ}$, thus leading to the highest magnitude of the excited state dipole moment (Table 4) [31]. Moreover, the ICT2 conformer with $\varphi = 90^{\circ}$ is supposed to be further stabilized after the dye relaxation in polar solvents, compared to that with $\varphi = 37^{\circ}$, while increased solvation energy (which is proportional to μ_{S1}^{abs}) of the dye may reduce the TICT state energy level (Fig. 7A) [71,76]. In general, all probes showed similar dependences of the above photophysical properties on the torsion angle φ (Tables 3 and 4). Interestingly, these features are close to those found by Stsiapura et al. both for the non-relaxed (S_1^{abs}) and relaxed (S_1^{fluor}) excited states of ThT [24]. Therefore, the study of the photophysical properties of the ThT derivatives in the non-relaxed excited state can provide a good approximate picture of their fluorescence properties.

The above calculations indicate that the internal charge transfer does occur upon the excitation of ThT derivatives, and the dipole moments undergo significant changes (except of ICT3 and ICT5), leading, as a consequence, to possible formation of the TICT state, appeared at lower energy than the LE state [32]. Furthermore, the

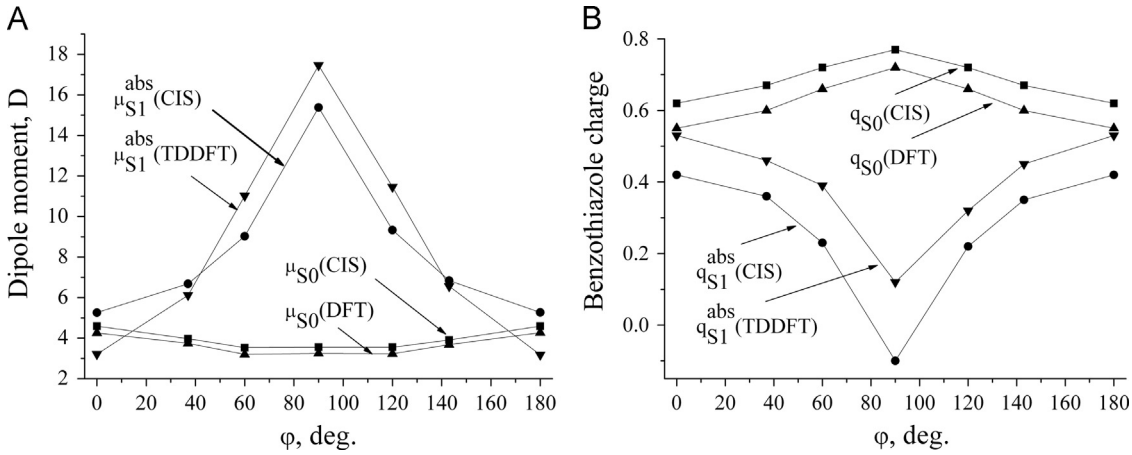

Fig. 8. Quantum chemical characteristics of the ground S_0 and first excited state S_1^{abs} of ICT2 conformers with different φ angles. Calculations were implemented using the ground state geometries optimized with the AM1 method, including an additional polarization function on H-atoms, 1 polarization and 1 diffuse functions on heavy atoms. Dipole moments (A) and benzothiazole charges (B) of the states $S_0(S_1^{abs})$ were obtained with DFT(TDDFT)/B3LYP/6-31G(d,p) or CIS/6-31G(d,p).

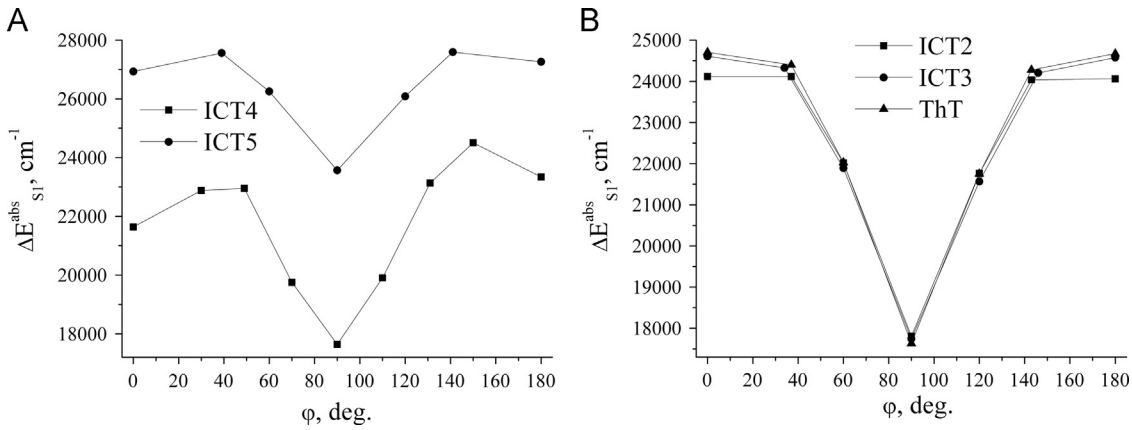

Fig. 9. The first excited state energies (ΔE_{S1}^{abs}) of ICT4, ICT5 (A) and ICT2, ICT3, ThT (B) conformers with different φ angles. Calculations were performed using the ground state geometries optimized with the AM1 method, including an additional polarization function on H-atoms, 1 polarization and 1 diffuse functions on heavy atoms. The energies were obtained with the TDDFT(B3LYP)/6-31G(d,p).

formation of the fully twisted conformations of the novel dyes upon excitation is plausible, since there exists a local minimum on the potential energy profile along the rotation of the phenyl ring with respect to the benzothiazole moiety (Fig. 7A). In turn, the TICT state seems to be nonfluorescent because of zero oscillator strengths for the $S_0 \rightarrow S_1^{abs}$ electronic transitions, which is also confirmed by the absence of the red-shifted second emission bands, corresponding to the TICT fluorescence of the dyes (Fig. 4, Table 2). Moreover, the TICT state cannot borrow intensity from higher vibronic levels of the allowed states due to the low energy levels of the excited TICT states of the dyes, which seem to be further reduced after relaxation of the probes in polar solvents [31,71].

3.4. Fluorescence properties of the Thioflavin T derivatives ICT4 and ICT5 are determined by the stabilization of the locally excited states upon excitation

Next, based on quantum-chemical calculations, we attempted to explain why the novel fluorophores, especially ICT4 and ICT5, have up to *ca.* 3880 times order higher fluorescence quantum yields in buffer solution compared to ThT (Table 1, Q_{buf}). As seen in Tables 3 and 4, the LE state energies of the examined dyes (except of ICT5) are lower than those of ThT, and the energies of the TICT state show the opposite behavior, suggesting higher stabilization of the partially twisted conformers and destabilization of the fully twisted conformers upon excitation, as was obtained, e.g., for another ThT analog, BTA-2, with INDO/S [25]. Notably, increase of the TICT energy level may occur due to the weaker electron-donating power of the phenyl ring substituents of ICT3 and ICT5, weaker electron-accepting ability of the benzothiazole moiety of ICT2, or steric restrictions in ICT4 [71,72]. Furthermore, the excited state energy profiles of the brightest probes, ICT4 and ICT5, were similar to that of BTA-2. Specifically, they had three directly observed minima, corresponding to the dye conformers with $\varphi=0$, $\varphi=180$ and $\varphi=90$, compared to the other fluorophores, possessing the minima only for the conformers with $\varphi=90$ (Fig. 9). The energy minima at $\varphi=0$ and $\varphi=180$ may correspond to the LE states of the dyes, i.e. they are assumed to adopt more planar conformation upon excitation. Furthermore, the values of the energy "humps" for the intramolecular rotation from $\varphi=0$ to $\varphi=90$ were *ca.* 1315 and 630 cm^{-1} for ICT4 and ICT5, respectively, exhibiting positive correlation with fluorescence quantum yields of the probes in buffer (Table 1, Q_{buf}). The reduced TICT state population of ICT4 and ICT5 is further corroborated by the fact, that the conformers with $\varphi=0$ and $\varphi=\varphi_{min}$ of the brightest dyes have the lowest f values (Table 3). Obviously, the LE states of ICT2 and ICT3 play an important role in the photophysics of these probes, although they are less stable than those of ICT4 and ICT5, and seem to be located on the energy plateau, corresponding to the conformers with $\varphi=0-40^{\circ}$ or $\varphi=140-180^{\circ}$ (Fig. 9B) [25].

This may account for weaker fluorescence of ICT2 and ICT3 in buffer solution compared to ICT4 and ICT5 (Table 1, I_0). Finally, the obtained energy barriers for the rotational isomerization should increase if they are calculated for the relaxed excited states of the dyes, because the novel fluorophores turned out to be much brighter than ThT. Notably, ICT3 showed the most similar excited state energy profile to that of ThT (Fig. 9B). This could explain the lowest stability of the dye LE state (Table 1, I_{buf}) and the highest "light-up" ability of ICT3 in the presence of insulin amyloid fibrils as compared to the other probes under study.

In turn, high stability of the LE states implies low sensitivity of a dye to microenvironmental viscosity [77,78] that was indeed observed experimentally for the ThT derivatives as compared to ThT (Table 1, I_{GL}/I_{DMF}). Interestingly, similar results were reported, e.g., for BTA-0, BTA-1 and BTA-2, possessing bright fluorescence in buffer solution, lower "light-up" abilities in the presence of Aβ fibrils, and, surprisingly, stronger affinity for the protein aggregates [16]. The above data suggest that the photophysical properties of the studied ThT analogs are determined by the stable LE states of these fluorophores. Specifically, the energy barriers for the formation of fully twisted state observed for the novel dyes may arise from at least three factors: (i) sterical constraints for rotational isomerization of the probes [75,77]; (ii) lower ground state dipole moments of the LE state compared to those of TICT state [24]; and (iii) weaker changes of the dipole moments upon excitation [32]. Indeed, steric interactions between the bulky substituent on the benzothiazole ring and H-atoms of the phenyl moiety of ICT4 may restrict the intramolecular rotation of the dye [75]. Besides, ICT4 may prefer the non-twisted conformation in the excited state due to very high μ_{S1}^{abs} value at $\varphi = \varphi_{min}$. In turn, the ground state dipole moments of ICT3 and ICT5 at $\varphi = \varphi_{min}$, which are lower than those at $\varphi = 90$, along with the lowest change of these values upon excitation may account for stability of the LE states of the ThT derivatives (Tables 3 and 4) [24,32]. Finally, ICT2 showed the increased μ_{S0} value, compared to that of ThT, presumably inducing stabilization of the locally excited state [33].

Taken together, ICT2 and ICT3 turned out to have comparable photo-chemical properties and spectral responses to the presence of insulin (lysozyme) aggregates with ThT. In turn, higher stability of the LE states of ICT4 and ICT5 derivatives in buffer solution resulted in a significant reduction of their "light-up" abilities compared to ThT. Presumably, ICT4 and ICT5 could be employed as laser dyes (e.g., in a mixture with other laser dyes with the purpose of tuning range broadening) due to the very high quantum yields in buffer solution [79,80].

4. Conclusions

To summarize, the present study showed that the four ThT derivatives, especially ICT2 and ICT5, could be employed for distinguishing amyloid fibrils of varied polarity *in vitro* due to the difference of their emission maxima in insulin- and lysozyme-bound states. In turn, ICT2 and ICT3 have a potential to be used for amyloid detection and distinguishing between the protein aggregates of different viscosity due to the high sensitivity of their fluorescence signals to the restricted intramolecular rotation. Finally, quantum-chemical calculations revealed that photophysical properties of ICT4 and ICT5 are determined by the stable locally excited states, since the formation of the twisted intramolecular charge transfer states is suppressed compared to ThT, ICT2 and ICT3, due to the steric constraints or slight changes in the dipole moments of the dyes upon excitation. This resulted in the bright fluorescence of the probes in buffer solution and weak fluorescence response in the presence of insulin and lysozyme protein aggregates.

Acknowledgment

This work was supported by the Grant from Fundamental Research State Fund (Project no. F.54.4/015) and CIMO Fellowship (Grants' no. TM-13-8785 and TM-14-9254).

References

[1] B. Caughey, P.T. Lansbury, Annu. Rev. Neurosci. 26 (2003) 267.
[2] D.J. Selkoe, Nature 426 (2003) 900.
[3] B.H. Toyama, J.S. Weissman, Annu. Rev. Biochem. 80 (2011) 557.
[4] J. Greenwald, R. Riek, Structure 18 (2010) 1244.
[5] J.T. Meijer, M. Roeters, V. Viola, D.W. Lowik, G. Vriend, J.C. van Hest, Langmuir 23 (2007) 2058.
[6] M.R. Nilsson, Methods 34 (2004) 151.
[7] O.S. Makin, L.C. Serpell, Methods Mol. Biol. 299 (2005) 67.
[8] A. Hawe, M. Sutter, W. Jiskoot, Pharm. Res. 25 (2008) 1487.
[9] S.G. Bolder, L.M. Sagis, P. Venema, E. van der Linden, Langmuir 23 (2007) 4144.
[10] A.A. Maskevich, V.I. Stsiapura, V.A. Kuzmitsky, I.M. Kuznetsova, O.I. Povarova, V.N. Uversky, K.K. Turoverov, J. Proteome Res. 6 (2007) 1392.
[11] C. Wu, V.W. Pike, Y. Wang, Curr. Top. Dev. Biol. 70 (2005) 171.
[12] C.A. Mathis, B.J. Bacskai, S.T. Kajdasz, M.E. McLellan, M.P. Frosch, B.T. Hyman, D.P. Holt, Y. Wang, G.F. Huang, M.L. Debnath, W.E. Klunk, Bioorg. Med. Chem. Lett. 12 (2002) 295.
[13] R. Leuma Yona, S. Mazeres, P. Faller, E. Gras, ChemMedChem 3 (2008) 63.
[14] C.A. Mathis, Y. Wang, D.P. Holt, G.F. Huang, M.L. Debnath, W.E. Klunk, J. Med. Chem. 46 (2003) 2740.
[15] K. Cisek, J. Kuret, Bioorg. Med. Chem. 20 (2012) 1434.
[16] W.E. Klunk, Y. Wang, G.F. Huang, M.L. Debnath, D.P. Holt, C.A. Mathis, Life Sci. 69 (2001) 1471.
[17] C. Wu, M.T. Bowers, J.E. Shea, Biophys. J. 100 (2011) 1316.
[18] J. Ali-Torres, A. Rimola, C. Rodriguez-Rodriguez, L. Rodriguez-Santiago, M. Sodupe, J. Phys. Chem. B 117 (2013) 6674.
[19] L. Qin, J. Vastl, J. Gao, Mol. Biosyst. 6 (2010) 1791.
[20] A.D. Cohen, G.D. Rabinovici, C.A. Mathis, W.J. Jagust, W.E. Klunk, M.D. Ikonomovic, Adv. Pharmacol. 64 (2012) 27.
[21] A. Lockhart, L. Ye, D.B. Judd, A.T. Merritt, P.N. Lowe, J.L. Morgenstern, G. Hong, A.D. Gee, J. Brown, J. Biol. Chem. 280 (2005) 7677.
[22] W.A. Banks, BMC Neurol. 9 (Suppl. 1) (2009) S3.
[23] J.R. Lakowicz, Principles of Fluorescence Spectroscopy, third ed., Springer, New York, 2006.
[24] V.I. Stsiapura, A.A. Maskevich, V.A. Kuzmitsky, K.K. Turoverov, I.M. Kuznetsova, J. Phys. Chem. A 111 (2007) 4829.
[25] V.I. Stsiapura, A.A. Maskevich, V.A. Kuzmitsky, V.N. Uversky, I.M. Kuznetsova, K.K. Turoverov, J. Phys. Chem. B 112 (2008) 15893.
[26] A.I. Sulatskaya, A.A. Maskevich, I.M. Kuznetsova, V.N. Uversky, K.K. Turoverov, PloS ONE 5 (2010) e15385.
[27] M. Biancalana, S. Koide, Biochim. Biophys. Acta. 2010 (1804) 1405.
[28] M.A. Haidekker, T.P. Brady, D. Lichlyter, E.A. Theodorakis, Bioorg. Chem. 33 (2005) 415.
[29] R. Mishra, D. Sjolander, P. Hammarstrom, Mol. Biosyst. 7 (2011) 1232.
[30] M. Nepraš, O. Machalický, M. Šeps, R. Hrdina, P. Kapusta, V. Fidler, Dyes Pigment. 35 (1997) 31.
[31] M.A. Haidekker, E.A. Theodorakis, J. Biol. Eng 4 (2010) 11.
[32] M.A. Haidekker, M. Nipper, A. Mustafic, D. Lichlyter, M. Dakanali, E.A. Theodorakis, Dyes with segmental mobility: molecular rotors, in: A.P. Demchenko (Ed.), Advanced Fluorescence Reporters in Chemistry and Biology I: Fundamentals and Molecular Design, vol. 8, Springer Ser Fluoresc, Springer-Verlag, Berlin Heidelberg, 2010, pp. 267–308, http://dx.doi.org/10.1007/978-3-642-04702-2_8.
[33] E.S. Voropai, M.P. Samtsov, K.N. Kaplevskii, A.A. Maskevich, V.I. Stepuro, O.I. Povarova, I.M. Kuznetsova, K.K. Turoverov, A.L. Fink, V.N. Uverskii, J. Appl. Spectrosc. 70 (2003) 868.
[34] V. Foderà, M. Groenning, V. Vetri, F. Librizzi, S. Spagnolo, C. Cornett, L. Olsen, M. van de Weert, M. Leone, J. Phys. Chem. B 112 (2008) 15174.
[35] R. Sabate, I. Lascu, S.J. Saupe, J. Struct. Biol. 162 (2008) 387.
[36] T.G. Deligeorgiev, Dyes Pigment. 12 (1990) 243.
[37] T. Deligeorgiev, A. Vasilev, S. Kaloyanova, J.J. Vaquero, Color. Technol. 126 (2010) 55.
[38] M. Groenning, M. Norrman, J.M. Flink, M. van de Weert, J.T. Bukrinsky, G. Schluckebier, S. Frokjaer, J. Struct. Biol. 159 (2007) 483.
[39] K. Sasahara, H. Yagi, H. Naiki, Y. Goto, J. Mol. Biol. 372 (2007) 981.
[40] K. Vus, V. Trusova, G. Gorbenko, E. Kirilova, G. Kirilov, I. Kalnina, P. Kinnunen, Chem. Phys. Lett. 532 (2012) 110.
[41] H. LeVine 3rd, Protein Sci. 2 (1993) 404.
[42] K.D. Volkova, V.B. Kovalska, A.O. Balanda, M.Y. Losytskyy, A.G. Golub, R.J. Vermeij, V. Subramaniam, O.I. Tolmachev, S.M. Yarmoluk, Bioorg. Med. Chem. 16 (2008) 1452.
[43] M. Girych, G. Gorbenko, V. Trusova, E. Adachi, C. Mizuguchi, K. Nagao, H. Kawashima, K. Akaji, S. Lund-Katz, M.C. Phillips, H. Saito, J. Struct. Biol. 185 (2014) 116.
[44] M.J.S. Dewar, E.G. Zoebisch, E.F. Healy, J.J.P. Stewart, J. Am. Chem. Soc. 107 (1985) 3902.

[45] S. Gonta, M. Utinans, G. Kirilov, S. Belyakov, I. Ivanova, M. Fleisher, V. Savenkov, E. Kirilova, Mol. Biomol. Spectrosc. 101 (2013) 325.
[46] A.-D. Gorse, M. Pesquer, J. Phys. Chem. 99 (1995) 4039.
[47] J.S. Binkley, J.A. Pople, W.J. Hehre, J. Am. Chem. Soc. 102 (1980) 939.
[48] R.G. Parr, W. Yan, Density-Functional Theory of Atoms and Molecules, Oxford University Press, Oxford, 1989.
[49] S. Scheiner, J. Phys. Chem. A 104 (2000) 5898.
[50] E. Runge, E.K.U. Gross, Phys. Rev. Lett. 52 (1984) 997.
[51] J.B. Foresman, M. Head-Gordon, J.A. Pople, M.J. Frisch, J. Phys. Chem. 96 (1992) 135.
[52] J.F. Stanton, J. Gauss, N. Ishikawa, M. Head-Gordon, J. Chem. Phys. 103 (1995) 4160.
[53] R.J. Cave, K. Burke, E.W. Castner, J. Phys. Chem. A 106 (2002) 9294.
[54] F. Furche, R. Ahlrichs, J. Chem. Phys. 117 (2002) 7433.
[55] M. Jaworska, G. Kazibut, P. Lodowski, J. Phys. Chem. A 107 (2003) 1339.
[56] M.W. Schmidt, K.K. Baldridge, J.A. Boatz, S.T. Elbert, M.S. Gordon, J.H. Jensen, S. Koseki, N. Matsunaga, K.A. Nguyen, S. Su, T.L. Windus, M. Dupuis, J.A. Montgomery, J. Comput. Chem. 14 (1993) 1347.
[57] B.M. Bode, M.S. Gordon, J. Mol. Graph. Model. 16 (1998) 133.
[58] J. Murali, R. Jayakumar, J. Struct. Biol. 150 (2005) 180.
[59] R. Amini, R. Yazdanparast, S. Bahramikia, Int. J. Biol. Macromol. 60 (2013) 334.
[60] S.S. Wang, K.N. Liu, Y.C. Lu, Biochem. Biophys. Res. Commun. 381 (2009) 639.
[61] I.M. Kuznetsova, A.I. Sulatskaya, V.N. Uversky, K.K. Turoverov, PLoS ONE 7 (2012) 2.
[62] L.S. Wolfe, M.F. Calabrese, A. Nath, D.V. Blaho, A.D. Miranker, Y. Xiong, Proc. Natl. Acad. Sci. USA 107 (2010) 16863.
[63] T.P.J. Knowles, T.W. Oppenheim, A.K. Buell, D.Y. Chirgadze, M.E. Welland, Nat. Nanotechnol. 5 (2010) 204.
[64] T.P. Knowles, A.W. Fitzpatrick, S. Meehan, H.R. Mott, M. Vendruscolo, C.M. Dobson, M.E. Welland, Science 318 (2007) 1900.
[65] J. Adamcik, A. Berquand, R. Mezzenga, Appl. Phys. Lett. 98 (2011) 193701.
[66] E. Kachooei, A.A. Moosavi-Movahedi, F. Khodagholi, H. Ramshini, F. Shaerzadeh, N. Sheibani, PLoS ONE 7 (2012) e41344.
[67] J.L. Jimenez, E.J. Nettleton, M. Bouchard, C.V. Robinson, C.M. Dobson, H.R. Saibil, Proc. Natl. Acad. Sci. USA 99 (2002) 9196.
[68] S.E. Hill, T. Miti, T. Richmond, M. Muschol, PLoS ONE 6 (2011) e18171.
[69] J. Adamcik, J.-M. Jung, J. Flakowski, P. De Los Rios, G. Dietler, R. Mezzenga, Nat. Nanotechnol. 5 (2010) 423.
[70] Z.R. Grabowski, K. Rotkiewicz, W. Rettig, Chem. Rev. 103 (2003) 3899.
[71] W. Rettig, Angew. Chem. Int. Ed. Engl. 25 (1986) 971.
[72] W. Rettig, M. Zander, Chem. Phys. Lett. 87 (1982) 229.
[73] G.J. Zhao, K.L. Han, J. Comput. Chem. 29 (2008) 2010.
[74] L.M. Daku, J. Linares, M.L. Boillot, Phys. Chem. Chem. Phys. 12 (2010) 6107.
[75] S. Keinan, E. Zojer, J.L. Bredas, M.A. Ratner, T.J. Marks, J. Mol. Struct. (Theochem) 633 (2003) 227.
[76] G. Scalmani, M.J. Frisch, B. Mennucci, J. Tomasi, R. Cammi, V. Barone, J. Chem. Phys. 124 (2006) 94107.
[77] J. Sutharsan, D. Lichlyter, N.E. Wright, M. Dakanali, M.A. Haidekker, E.A. Theodorakis, Tetrahedron 66 (2010) 2582.
[78] A.S. Klymchenko, G. Duportail, A.P. Demchenko, Y. Mely, Biophys. J. 86 (2004) 2929.
[79] V.V. Maslov, Funct. Mater. 19 (2012) 226.
[80] A.H. Abdelrahman, M.A. Abdelrahman, M.K. Elbadawy, Nat. Sci. 5 (2013) 1183.